JThA46.pdf

Implant Enhanced Dual Intracavity Polarization Switching Asymmetric Current Injected VCSEL

Yan Zheng[†], Chin-Han Lin[†] and, Larry A. Coldren[†*]
[†]Department of Electrical and Computer Engineering
[*]Department of Materials
University of California, Santa Barbara 93106

Abstract

Output polarization is controlled by injecting current along crystalline directions. VCSELs with record-low threshold current of 0.19 mA and extinction ratio >21dB from fit is achieved. Polarization switching is shown to be enhanced by implantation.

OCIS codes: 140.7260 Vertical cavity surface emitting lasers, 130.5440 Polarization-selective devices

I. Introduction

Meeting the needs of next-generation computational systems and data centers will require a concerted effort on many different fronts. Vertical-cavity surface-emitting lasers (VCSELs) have emerged in this effort as a valuable platform because of their reliability, high speed characteristics, and their ability for onchip integration of components such as microlenses. Recently our group has demonstrated 980 nm VCSELs capable of 35Gb/s error-free operation with a very low-threshold of only 0.144 mA [1]. Still, other avenues such as polarization control can be explored for other innovative approaches. For instance, output polarization control can increase the bit/symbol density by additionally embedding polarization information. Other work has also demonstrated 40Gb/s NRZ optical memory using a polarization bistable VCSEL [2].

Although polarization stability has been demonstrated using various geometries, off-axis crystal surfaces, and surface gratings [3]-[5], these devices lose the functionality that comes with complete output polarization control. Recently several groups have investigated asymmetric current injection (ACI) as a way to introduce gain anisotropy to control output polarization [6]-[7]. We demonstrate switching between two orthogonal polarization states via asymmetric current injection utilizing a novel dual intracavity contacted circular mesa design. A record-low threshold current of 0.19 mA was achieved. Deuterium (D^+) implantation in the p-contact layer was also investigated to reduce lateral current spreading.

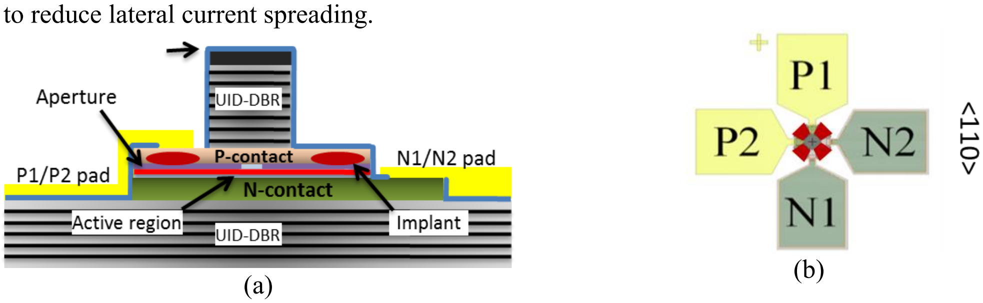

Fig. 1 a) Polarization switching VCSEL schematic. b) Top view showing contact pads relative to <110>. Ion implant locations shown in red.

II. Growth and Fabrication

Devices were grown using molecular beam epitaxy (MBE) on undoped (001) GaAs starting with 18 periods of GaAs/AlAs to form the bottom DBR mirror followed by 420nm of Si doped GaAs for the n-contact layer. The p- and n-contact layers were grown close together to increase current directionality. The active region consists of three 8nm thick $In_{0.2}G_{0.8}As$ quantum wells separated by 8nm GaAs barriers surrounded by a 30% AlGaAs separate confinement heterostructure (SCH). A linearly graded AlGaAs region then forms the oxide aperture. A modulation carbon doped GaAs p-contact layer is grown followed by 32 periods of 85% AlGaAs/GaAs to form the top mirror.

Circular mesas were created in a two-step dry-etch process that stops in the intracavity contact layers using a laser etch-monitor. An oxide aperture was created and a third etch removes the n-contact layer except from where the n-metal pads will be to help isolate orthogonal electron paths. A blanket SiN layer is deposited and four equally spaced vias are opened around the mesa for metal contacts. The pad layout, shown in Fig. 1b is designed to break the conventional current injection symmetry and increase current directionality. Above threshold where there is sufficient state filling, current direction is used to provide a significant lateral carrier momentum component to control output polarization. Deuterium was also implanted into the p-contact layer in areas that straddle current injection paths shown in Fig. 1.

III. Experimental Results

Light output (LI) first passes through a rotating polarizing lens and then is measured by a Si photodetector. The polarizer transmission axis is aligned to the 0° marker on the rotational mount which is then aligned, by eye, to the <1$\bar{1}$0> axis of the wafer.

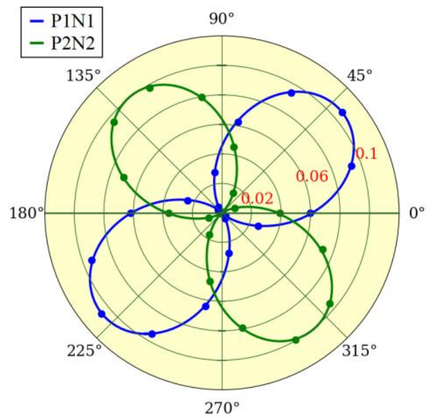

Fig. 2 Output power (radii-a.u.) and polarizer angle at 2.0 mA for the P1N1 and P2N2 current directions. 0° is aligned to the <1$\bar{1}$0> axis.

LI curves were taken for every 20° rotation of the polarizer with either the P1N1 or P2N2 configuration probed. Light output of the device at a bias of 2 mA is plotted against the polarizer rotation angle to generate the polarization resolved polar plot shown in Fig. 2. Two polarization states are clearly shown with a phase offset of approximately 90°. The measured data fit very well to a sine wave with a R^2 value >0.999 and both showing a polarization rotational frequency of 2rad^{-1}. From the fit, record extinction ratios >21dB between polarization states were achieved at a bias of 2 mA.

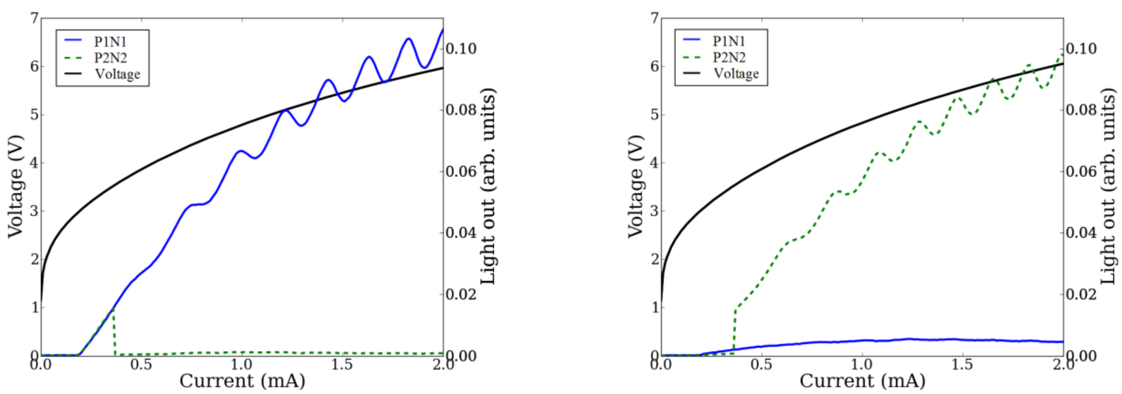

(a) (b)

Fig. 3 LIV curves for orthogonal current directions with polarizer transmission axis a) 40° to the <1$\bar{1}$0> axis b) and 120° to the <1$\bar{1}$0> axis.

CW LIV curves for two polarization states under asymmetric current injection conditions are shown in Fig. 3. A typical IV curve shows a turn-on voltage of 1.7 V and is smooth when the polarization switches and throughout the rest of the current range. The threshold current of 0.19 mA is the lowest reported for an ACI VCSEL. Light output was found to be polarized close to 40° from the <1$\bar{1}$0> axis when biasing the P1N1 pads. The output from biasing the P2N2 pads has the same polarization up until 0.37 mA where it then switches polarization and is almost completely extinguishing. At a polarizer angle of 120°, LI curves taken for both the P1N1 and P2N2 current injection directions are mirror opposites of that seen at 40°, shown in Fig. 3(b). The P2N2 output is slightly higher because the data was not taken at the optimal polarization splitting angle. Ripples in the light output are believed to be from local heating and which disappear under 1 μs pulsed conditions.

The enhancement of polarization switching from implantation is illustrated in Fig. 4. For a device that did not show polarization splitting from ACI, when implanted with D^+, the output polarization showed a polarization phase offset of approximately 90°. The P2N2 polarization state slightly rotates clock-wise while the P1N1 state rotates in the counter clock-wise direction. Increased loss from the implant is suspected to be the cause of the slight reduction in output power.

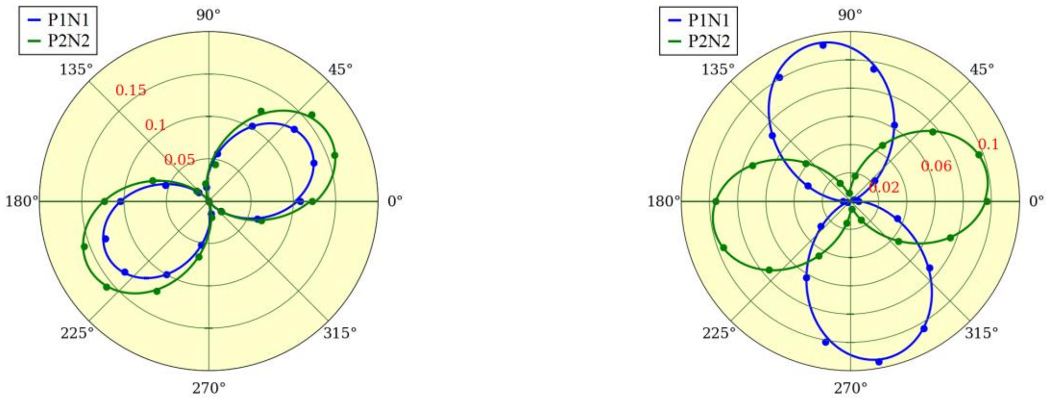

(a) (b)

Fig. 4 Output power (radii-a.u.) and polarizer angle for the P1N1 and P2N2 current directions of a device a) before D^+ implantation and b) after D^+ implant. The 0° horizontal axis is aligned to the crystalline <1$\bar{1}$0> axis.

V. Conclusion

A VCSEL capable of controlled switching between polarization states by changing the direction of current injection was demonstrated. The measured threshold current of 0.19 mA is the lowest reported for an asymmetric current injection polarization switching VCSEL. Output polarization profile was fit to a sine wave where a record high extinction ratio of >21dB was obtained between orthogonal polarization states. Deuterium implantation was also shown to enhance polarization splitting.

VI. Acknowledgements

This work was supported by DARPA through a STTR with Ziva Corporation.

VII. References

[1] Y.-C. Chang and L.A. Coldren, "High-efficiency, high-speed VCSELs for optical interconnects," *Applied Physics A*, **95**(4), pp.1033-1037, June 2009.

[2] J. Skaguchi, T. Katayama, H. Kawaguchi, "All-optical memory operation of 980-nm polarization bistable VCSEL for 20-Gb/s PRBS RZ and 40-Gb/s NRZ data signals," *Optics Express*, **18**(12), pp. 12362-12370, June 2010.

[3] K. D. Choquette and R. E. Leibenguth, "Control of vertical cavity polarization with anisotropic transverse cavity geometries," *IEEE Photonic Technol. Lett.*, **6**, pp. 40 - 42, 1994.

[4] M. Takahashi, N. Egami, T. Mukaihara, F. Koyama, and K. Iga, "Lasing characteristics of GaAs(311)A substrate based InGaAs-GaAs vertical-cavity surface-emitting lasers", *IEEE J. Select. Topics Quantum Electron.*, **3**, pp. 372 - 378, 1997.

[5] J. M. Ostermann, P. Debernardi and R. Michalzik, "Optimized integrated surface grating design for polarization-stable VCSELs," *IEEE J. Quantum Electron.*, **42**, pp. 690, 2006.

[6] L.M. Augustin, E. Smalbrugge, K.D. Choquette, et. al., *IEEE Photon. Technol. Lett*., **16 (**3), 708–710, Mar. 2004.

[7] H.P.D. Yang, I.C. Hsu, F.I. Lai, et. al., *Jpn. J. Appl. Phys,.* **46** (14), 326-329, 2007.